# Liquid-metal-jet anode electron-impact x-ray source

O. Hemberg,[a] M. Otendal, and H. M. Hertz
*Biomedical and X-ray Physics, Royal Institute of Technology, SE-106 91 Stockholm, Sweden*

(Received 27 March 2003; accepted 18 June 2003)

We demonstrate an anode concept, based on a liquid-metal jet, for improved brightness in compact electron-impact x-ray sources. The source is demonstrated in a proof-of-principle experiment where a 50 keV, ~100 W electron beam is focused on a 75 $\mu$m liquid-solder jet. The generated x-ray flux and brightness is quantitatively measured in the 7–50 keV spectral region and found to agree with theory. Compared to rotating-anode sources, whose brightness is limited by intrinsic thermal properties, the liquid-jet anode could potentially be scaled to achieve a brightness $>100\times$ higher than current state-of-the-art sources. Applications such as mammography, angiography, and diffraction would benefit from such a compact high-brightness source. © *2003 American Institute of Physics.* [DOI: 10.1063/1.1602157]

Compact electron-impact x-ray sources are widely used for diagnostics and imaging in medicine, industry, and science. A key figure of merit for such x-ray systems is the source brightness. Unfortunately the brightness is proportional to the electron-beam power density ($W/mm^2$) at the anode, and current rotating-anode and microfocus technology show little potential for further improvement due to intrinsic thermal limitations.[1,2] In this letter we introduce an anode concept, based on a liquid-metal jet, which has potential to increase the brightness $>100\times$ due to inherently different thermal limitations.

Medical diagnostics,[1,2] such as mammography (~20 keV) or angiography (~60 keV), and protein structure determination based on x-ray diffraction[3] (~10 keV) are important applications of modern x-ray technology. In both cases the brightness [e.g., photons/($mm^2$ sr s BW)] is the important source parameter. In medical imaging a smaller source at constant flux (photons/s) results in higher-resolution imaging since this is basically a shadow-type imaging system not limited by diffraction. In crystallography, a higher brightness allows faster measurements on smaller samples. Therefore, crystallography has been greatly aided by the significant increase in brightness of synchrotron radiation sources in the last decades.

For compact hard x-ray sources, however, the development as regards brightness has been slow. These sources are based on the emission of bremsstrahlung and characteristic line radiation from decelerating kilo-electron-volt electrons in a solid-target-material anode. The conversion efficiency from electron-beam energy to x-ray energy is typically in the $<1\%$ range. Soon after Röntgen's original work it was clear that thermal effects at the anode limited the x-ray flux as well as the brightness. Since then, the only major invention is the rotating anode in the 1930:s. Improvements in speed of rotation, cooling, materials, etc., now allows 10–15 $kW/mm^2$ electron-beam power density on the anode. However, all modern x-ray tubes use the line-focus principle and angled viewing of the anode to decrease the effective x-ray spot size $\sim 10\times$.[2] This factor must not be forgotten when comparing the actual power load capacity of different anodes although the real gain in performance is reduced somewhat by, e.g., the Heel effect.[1] Thus, the effective electron-beam power density increases correspondingly to 100–150 $kW/mm^2$. Typical high-end implementations are, e.g., 10 kW, 0.3 mm effective x-ray spot size angiography systems and 1.5 kW, 0.1 mm effective x-ray spot size fine-focus mammography systems.[1,2] Low-power microfocus sources[4] (4 W, 5 $\mu$m effective x-ray spot size) have similar effective power densities (200 $kW/mm^2$) and are also limited by thermal effects.

In the present letter we demonstrate a type of anode which potentially allows $>100\times$ higher effective brightness, compared to current rotating-anode sources. The anode is based on a liquid-metal jet. As is shown later, the hydrodynamic and thermal properties of such a regenerative-jet anode allow for a much higher thermal load than rotating anodes. Basically, higher anode speed accounts for one order of magnitude and a higher thermal load limit for another order of magnitude. Also, the choice of target material is changed to low, rather than high, melting-point materials. Fortunately this is no major limitation but in some cases rather an advantage, since materials such as, e.g., Sn and Ga have significant line emission suitable for, e.g., mammography and x-ray crystallography, respectively. Liquid-jet target systems have previously been successfully demonstrated as laser-plasma target for negligible-debris high-brightness soft x-ray and extreme ultraviolet sources.[5,6] The concept has also been extended to hard x-ray generation using a liquid-gallium-jet as target for a femtosecond laser-plasma source.[7] Furthermore, electron beams have been combined with water liquid jets for low-power soft x-ray generation via fluorescence.[8]

The proof-of-principle experimental arrangement demonstrating the new source at low power is shown in Fig. 1. It basically consists of a liquid-metal-jet system and a focused electron-beam system in a vacuum chamber pumped to $\sim 10^{-5}$ mbar by a 500 l/s turbodrag pump. The electron beam is focused onto the liquid-metal jet resulting in x-ray generation. A laser flash photography system is used for jet characterization and an x-ray detection system for calibrated measurements of the generated x rays.

Metals are the preferred liquid-jet material for this appli-

[a]Electronic mail: oscar.hemberg@biox.kth.se

 

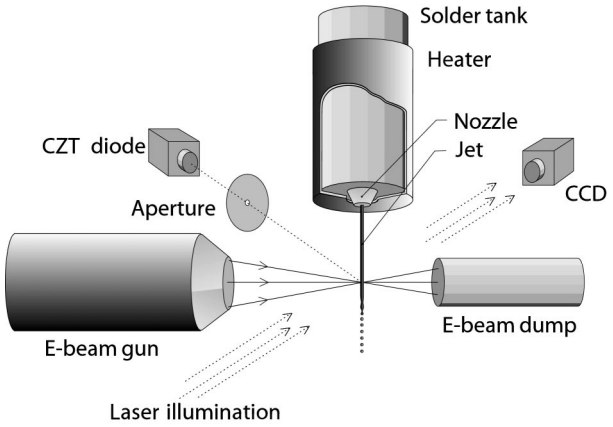


FIG. 1. Experimental arrangement of the liquid-metal-jet anode x-ray source proof-of-principle experiment.

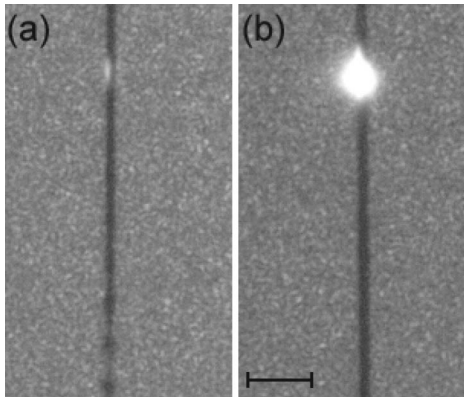


FIG. 2. Flash photograph (scale bar is 0.5 mm) of a ~75 $\mu$m tin jet targeted by ~150 $\mu$m FWHM electron beam. (a) ~0.5 W, low-speed operation with visible Rayleigh drop breakup. (b) Stable high-speed operation with ~100 W electron-beam power.

cation due to their high electric conductivity, high heat load capability and high *Z*. The specific choice of material depends on the desired x-ray emission wavelength as well as the thermodynamic properties. As previously mentioned, the heat load capacity of the target is crucial for high brightness operation, and the material should therefore have a large temperature span between the melting and boiling point, high specific heat capacity, high density, and high heat of vaporization. Furthermore, it is preferable with low-melting-point materials which are not prone to oxidization or otherwise reactive or harmful. Although pure materials provide a ''clean'' x-ray spectra, alloys may have material properties that make them more suitable for metal-jet operation. For the present proof-of-principle experiment a 63% Sn, 37% Pb solder alloy (m.p. 183 °C) was used, which combines suitable thermodynamic properties with Sn x-ray line emission for mammography.

The liquid-metal-jet system consists of a 0.15 l high-pressure tank, a 75 $\mu$m ruby pin-hole nozzle, and a sintered stainless-steel particle filter. The high-pressure tank is enclosed in an IR radiation heater, designed to produce a minimal magnetic leak-field not to perturb the electron beam. The entire assembly is grounded to avoid local charge buildup. The 250 °C alloy liquid jet is ejected by applying up to 200 bars of nitrogen, resulting in a maximum jet speed of ~60 m/s.

A 20 Hz, 4 ns pulsed frequency-doubled Nd:YAG laser is used to backilluminate the jet, which is imaged by a 12× zoom microscope during operation. With this system the directional stability of the jet was measured to $<5\ \mu$m ~10 mm from the nozzle orifice.

The fluid dynamics of the liquid-metal jet will only be briefly described here. The state of such jets are often characterized by Reynolds and Ohnesorge numbers (Re and Oh, respectively).[9] The parameters for the present jet ($d = 75\ \mu$m, $\eta = 2.1\times10^{-3}$ Ns/m$^2$, $\sigma = 0.51$ N/m, $\rho = 8.0\times10^3$ kg/m$^3$, $v = 60$ m/s) result in Re$=1.7\times10^4$ and Oh $=3.8\times10^{-3}$. The relation of Re and Oh, conventionally used to characterize jets in air,[9] clearly puts the current jet well past the laminar limit, in the transition region to fully developed turbulent flow. Still, Fig. 2(a) with its visible Rayleigh drop breakup indicates a laminar flow mode. This is believed to be due to the lack of air friction forces on the jet when injected into the vacuum environment. A more comprehensive discussion of high-speed liquid-metal jets in vacuum is in preparation.[10]

The 50 kV electron-beam system is based on a flat single-crystal $LaB_6$ thermionic cathode, a single-lens aperture acceleration gap, and a magnetic lens to image the virtual point source resulting from the beam divergence induced by the anode opening. This simple design is possible since the perveance is $<10^{-9}$ A V$^{-3/2}$, making space-charge effects unimportant.[11] The working distance from the lens exit aperture is ~100 mm and the focal point can be moved several millimeters in any direction by adjusting the lens current and using *x* and *y* deflection coil pairs mounted after the lens. The electron-beam system is separately pumped by a 250 l/s turbodrag pump, and the anode and lens exit apertures make it possible to maintain a local vacuum pressure $<10^{-7}$ mbar during operation. The current electron beam performance is ~100 W in a ~150 $\mu$m full width at half maximum (FWHM) focal spot.

The x-ray detection system is a commercial CdZnTe diode system with a calibrated response in the desired energy range. The maximum recommended count rate is $\sim10^4$ cps, making it necessary to attenuate high-power sources in order not to saturate the detector. Instead of using an absorption filter the system uses thick tungsten collimators, allowing the real x-ray spectrum to be directly measured.

Figure 3 shows the spectra obtained at a 90° angle from the incident electron beam. The spectrum was measured with a 1 mm diameter pinhole and $8.3\pm0.4\ \mu$A absorbed electron-beam current. The combination of a large pinhole and low current was chosen for the calibrated measurement to eliminate possible errors due to alignment of the very-high-aspect-ratio pinhole (1:40) necessary for measurements at full electron-beam power. The absorbed current was measured by observing the difference in the current deposited in the beam dump with and without the jet in focus. The jet absorbed 42% of the electron beam and this value was used to calculate the electron beam focus to ~150 $\mu$m FWHM, assuming a Gaussian beam profile. Thus, the x-ray spot size is approximately a ~75 $\mu$m wide center cut-out of the electron beam spot. The data are given in brightness per absorbed current, i.e., photons/(mm$^2$ sr s A eV), and has been corrected for detector efficiency, air and Be-window absorp-

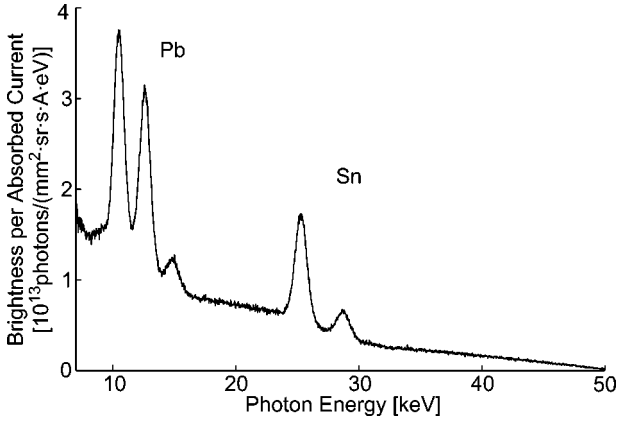


FIG. 3. X-ray spectrum from the proof-of-principle liquid-metal-jet anode x-ray source, showing the expected Pb *L* lines and Sn *K* lines on top of the continuous bremsstrahlung background.

tion, incident electron beam current, measurement geometry, and source size, and assuming uniform emission over $4\pi$ sr. The major uncertainty is in the source size and angular distribution, and the brightness data is estimated to be correct within $\pm 50\%$ in the measurement direction. The measured total bremsstrahlung yield above 7 keV was 0.19%, which compares well to the simple theoretical value of 0.20% for Sn and 0.32% for Pb.[12] The difference is believed to be due to the different target and measurement geometries including reabsorption of low-energy x rays in the jet. The system has been successfully operated with the present $\sim 100$ W maximum electron-beam power without any instabilities, as seen in Fig. 2(b). However, boiling and evaporation phenomena, in agreement with power load calculations, have been observed when using a high electron-beam power in combination with a low jet speed. Assuming the same absorption ratio and that the x-ray flux is proportional to the absorbed current, the achieved peak brightness in the present proof-of-principle experiment is $1.4\times 10^{10}$ photons/(mm$^2$ sr s eV) at the Sn $K_\alpha$ peak with an average electron-beam power density on the jet of $\sim 3$ kW/mm$^2$ within the FWHM of the spot.

Contrary to conventional anode technology, this liquid-metal-jet anode system is scalable to high-brightness operation. This is primarily due to the fact that a stable jet can be operated at a higher speed than a rotating anode (typically 60 m/s), and that the heat load capacity of the liquid jet is higher than that of a conventional anode due to its regenerative nature. For example, the power required to evaporate a 30 $\mu$m liquid-tin jet operated at 600 m/s is 9 kW, corresponding to an electron-beam density of 13 MW/mm$^2$ assuming a circular focus. This is $\sim 100\times$ higher than currently available effective power densities. Conceivably, this could be improved another factor $\sim 10\times$ if a flat jet with a perpendicular line focus is used, resulting in smaller effective x-ray spot. However, the system requires that a 9 kW ($<10^{-8}$ A V$^{-3/2}$) electron-beam must be focused to 30 $\mu$m or better. This appears possible, although the perpendicular line focus is on the theoretical limit with an acceptable working distance.[11] Experimentally, beams with similar perveance but with larger working distances and focal spots are found in current electron-beam welding technology.[13] As for the anode, a stable 30 $\mu$m, 600 m/s liquid-tin jet must be generated. Although this is in the classical spray-regime of liquid jets,[9,10] current water-jet cutting technology has demonstrated operation of sufficiently stable jets in this regime.[14]

Thus, two major challenges for high-brightness operation, the high-power-density electron-beam and the high-speed liquid-metal jet, appear achievable. The other main issue arises from the rapid heating of the jet during the $\sim 50$ ns transit time through the focused electron beam. It is not entirely clear how the jet will react to this rapid heating, nor what the ultimate power load limit is. However, there will be a vacuum issue due to evaporation. Since the thermal speed of the evaporated atoms will be comparable to the jet speed the jet should expand into a cone, thereby limiting the spot broadening and facilitating recovery of the jet. To protect the electron gun, differential pumping or a plasma window[15] may be necessary. Furthermore, the low-penetration depth of 50 keV electrons (a few microns) may lead to nonuniform heating in the jet due to the negligible thermal conduction during the $\sim 50$ ns transit time. Much of this problem could probably be alleviated by increasing the electron-beam voltage to better match the penetration depth and heat deposition to the jet diameter. Multiple electron beams would also provide a more uniform heating.

In conclusion, we have demonstrated a liquid-metal-jet anode electron-impact x-ray source that could potentially achieve 2–3 orders of magnitude increase in brightness compared to current compact sources. Several important applications would benefit from a higher brightness. Mammography and angiography are examples of high-resolution medical imaging whose performance today is limited by the source. Compact crystallography with reasonable resolution can be made available to the applied scientist. Finally, phase-contrast imaging using compact sources would be greatly aided by an increase in brightness.[16]

The authors thank Mikael Eriksson and Bengt Anderberg for their contributions. This work has been supported by the Swedish Agency for Innovation Systems and the Swedish Research Council.

[1] J. Beutel, H. L. Kundel, and R. L. Van Metter, *Handbook of Medical Imaging* (SPIE, Bellingham, WA, 2000), Vol. 1.
[2] E. Krestel, *Imaging Systems for Medical Diagnostics* (Siemens, Berlin, 1990).
[3] C. Giacovazzo, *Fundamentals of Chrystollagraphy* (Oxford University Press, New York, 1992).
[4] See, e.g., Thermo Kevex micro-focus source PXS5-926EA. (http://www.kevex.com).
[5] L. Rymell and H. M. Hertz, Opt. Commun. **103**, 105 (1993); L. Rymell, M. Berglund, and H. M. Hertz, Appl. Phys. Lett. **66**, 2625 (1995).
[6] B. A. M. Hansson, L. Rymell, M. Berglund, O. Hemberg, E. Janin, S. Mosesson, J. Thoresen, and H. M. Hertz, Proc. SPIE **4506**, 1 (2001).
[7] G. Korn, A. Thoss, H. Stiel, U. Vogt, M. Richardson, T. Elsaesser, and M. Faubel, Opt. Lett. **27**, 866 (2002).
[8] B. Buijsse, Proc. SPIE **4502**, 74 (2001).
[9] A. H. Lefebvre, *Atomization and Sprays* (Hemisphere, New York, 1989).
[10] M. Otendal *et al.* (unpublished).
[11] M. Sedlaček, *Electron Physics of Vacuum and Gaseous Devices* (Wiley, New York, 1996).
[12] B. K. Agarwal, *X-Ray Spectroscopy* (Springer, New York, 1991).
[13] See, e.g., Steigerwald EBOPULS G 120 PMS. (http://www.steigerwald-eb.de).
[14] D. A. Summers, *Waterjetting Technology* (Routledge, New York, 1995).
[15] A. Hershcovitch, Phys. Plasmas **5**, 2130 (1998).
[16] R. Fitzgerald, Phys. Today **53/7**, 23 (2000).